

High wind evaluation in the Southern Ocean

Xiaojun Yuan

Lamont-Doherty of Earth Observatory of Columbia University

61 Rt 9W, Palisades, NY 10964, (845) 365 8820, xyuan@ldeo.columbia.edu

Abstract

Space based scatterometer instruments provide crucial surface wind measurements with high resolution over global oceans. Mid-latitude regions in the Southern Ocean are unique places to evaluate scatterometer winds at high wind bands because these regions host the strongest wind fields at the ocean surface. The objective of this study is to evaluate QuikSCAT wind measurements by comparing them with reanalysis and weather station data in the Southern Ocean with an emphasis on high wind bands. The occurrence and intensity of high wind events in the scatterometer measurements are compared with that of reanalysis winds; and the spatial and seasonal variability of the high wind characteristics is examined. The results show that the speeds of scatterometer winds are comparable to model simulations in monthly mean field but consistently stronger than both ECMWF and NCEP/NCAR winds in high wind bands. When scatterometer winds are compared with the weather station observations at Macquarie Island, present study finds no systematic bias even at high wind bands. This suggests that model simulations may underestimate surface wind strength in high wind bands. Such underestimation would lead to up to 50% of reduction in energy fluxes between the atmosphere and ocean. Even though high winds occur only sporadically and the reanalysis underestimation in high wind speed is not in itself of great magnitude, they have a significant impact on global climate.

1. Introduction

The Southern Ocean is vital element in the global climate. Its circumpolar current plays a crucial role in the global transports of mass, heat and momentum, and transports climate signals from one ocean basin to another. Moreover, the Southern Ocean hosts the strongest surface winds of any open ocean area, fostering strong heat, moisture and momentum exchanges between ocean and atmosphere. However, the Southern Ocean is tremendously under-surveyed by traditional observation methods due to the remoteness of the area and rough environment, causing the largest data gap of global oceans. The data gap introduces large uncertainties into the data simulation of the region, both in global climate modeling and in estimating global energy budget. In the last two decades, satellite technologies have greatly enhanced our ability to monitor climate variables in this remote region, such as cloud, sea surface temperature, sea ice, surface height, surface wind and precipitation. These satellite observations play a critical role in modern climate studies.

Surface winds are crucial to determining many climate variables, such as heat, moisture and momentum fluxes between the atmosphere and ocean, mixed layer depth and Ekman transports, etc. They directly influence ocean circulation, water mass formations and energy transports between ocean basins. For more than a decade, space-based scatterometers have provided measurements of surface winds over global oceans with high spatial and temporal resolution (ERS-1/2, NSCAT, and QuikSCAT). In particular, QuikSCAT, a Ku-band scatterometer with a new design providing continuous 1,800 km swath, has been covering 93% of the global ocean daily with a within-swath spatial resolution of 25x25 km since September

1999 (Liu 2002). The accuracy of QuikSCAT has been improved compared to earlier scatterometers. The root-mean-square differences between collocated QuikSCAT and buoy measurements are 0.7 m/s for the speed and 13° for the direction under moderate conditions (Wentz et al. 2001). Validated by high quality wind observations from research vessels, Bourassa et al. (2003) showed that the uncertainties of QuikSCAT winds are 0.45 m/s and 5° for QSCAT-1 model function and 0.3 m/s and 3° for Ku-2000 model function. On the other hand, these validation studies were limited for the winds < 20 s/m. Whether these validations are applicable to the Southern Ocean, particularly in areas where winds could exceed 20 m/s due to strong westerly and frequent cyclone activities, remains unclear.

Historically, scatterometer measurements were subject to limitations on wind retrieval from backscatter under high wind conditions. A high-wind saturation was predicted by a theoretical study (e.g., Donelan and Pierson 1987). Such limitations were observed by NASA scatterometer (NSCAT) measuring tropical cyclones (Jones et al. 1999) and by scatterometers on aircraft for measuring wind speed higher than 20 m/s (Donnelly et al. 1999). QuikSCAT measurements also show considerable variation of backscatter as a function of wind at wind speed higher than 35 m/s (Yueh et al. 2000). However, recent studies show that backscatter measured by QuikSCAT is sensitive to wind variation at wind speeds as high as 50 m/s under clear-sky condition (Wentz et al. 2001) and during tropical cyclones at various rain rates (Yueh et al. 2001).

The objectives of this study are to cross-examine QuikSCAT winds against other wind products in the Southern Ocean from 30°S to ice edge, where the strong westerly prevails, and to

evaluate the impact of scatterometer winds on the estimation of cyclone activities and surface momentum flux. Because of the remoteness and rough environment, the region lacks ground truth data, such as buoy and ship measurements, presenting a tremendous challenge to wind evaluation. In cross-examining QuikSCAT winds against NCEP/NCAR reanalysis and ECMWF operational archive surface winds over the open Southern Ocean, this study finds discrepancies between the simulated winds and satellite observations. Wind observations from the Macquarie Island Weather Station are then used as ground truth measurements to evaluate both scatterometer winds and simulated winds.

2. Data and processes

Scatterometer winds

In this study, we use two QuikSCAT products: level 2 swath data by QSCAT-1 model function available from the Physical Oceanography Distributed Active Archive Center at the Jet Propulsion Laboratory, and swath data produced by the Ku-2001 geophysical model function (Wentz et al. 2001) from the Remote Sensing System. QSCAT-1 scatterometer winds (QSCAT-JPL, hereafter) are research quality data. We choose to use selected ambiguity in retrieving QSCAT-JPL winds. The Ku-2001 model function (QSCAT-RSS, hereafter) is an improved version of Ku-2000 model function, with better accuracy in retrieving winds higher than 20 m/s. Based on ship observations, the uncertainties of QuikSCAT wind speed and wind direction are 0.45 m/s and 5° for QSCAT-JPL products and 0.3 m/s and 3° for QSCAT-RSS products (Bourassa et al. 2003). QuikSCAT contains up to 76 cells across the satellite swath. Due to larger

uncertainties in the inner swath (< 200 km from nadir) and outer swath (> 700 km from nadir) (Bourassa et al. 2003), eight outer cells at each side of the swath and eighteen cells in the inner swath are excluded. One challenge for QuikSCAT wind retrieval is the rain contamination, which didn't significantly influence wind retrievals from earlier scatterometers (Sharp et al. 2002). To avoid the rain contamination, we also exclude wind cells with any rain flag.

Selected QuikSCAT swath winds from September 1999 to December 2000 are averaged into $1^\circ \times 1^\circ$ degree grid at a 12-hour temporal interval. A 3-dimensional interpolator (Zeng and Levy 1995) is then applied to fill spatial/temporal gaps. To fill a missing data point, the 3-dimensional interpolator uses data within a circle of 450 km radius weighted by the distance to the missing data point, as well as considers data within 3 time intervals centered at the time when the missing data occurs. The interpolator is also applied as a filter for all grid points to reduce the noise generated by ambiguity in wind direction. Such interpolated/filtered 12-hourly wind fields are then averaged to yield daily $1^\circ \times 1^\circ$ gridded data, which are cross-examined with daily simulated winds.

Simulated winds

In this study we use 10m winds from both ECMWF operational archive surface analysis data (Trenberth 1992, Trenberth et al. 1993) and NCEP/NCAR reanalysis products (Kalnay et al. 1996, Kistler, et al. 2001) in this study. The NCEP/NCAR reanalysis, producing daily 10m winds at a Gaussian grid with a resolution of 1.875° (approximately 210 km), is interpolated into a $1^\circ \times 1^\circ$ grid. The ECMWF analysis, which provides six hourly 10m winds at a Gaussian grid

with a resolution about 1.125° , is also interpolated and averaged into daily $1^\circ \times 1^\circ$ grid to be consistent with NCEP/NCAR and QuikSCAT winds.

Weather station data

The data from the Macquarie Island Weather Station ($54^\circ 30'S$, $158^\circ 57'E$) are chosen as ground truth in this study for the following reasons. Because the size of the Island (34 km long and 5 km wide at its widest point) is rather small compared to the satellite footprint, so it is unlikely that its existence influences surface winds in the surrounding waters. Also, the Island is located in the mean westerly zone, where strong winds prevail. This hilly island has no trees. In addition, the Australia Antarctic Station is located on the Island's northern tip -- surrounded by a marine environment. The hills in most parts of the Island have the least impact on the local surface winds at the station. The elevation of the station is 6m, close to the sea level. Adjustment of anemometer height to the height of 10m equivalent neutral winds (Liu and Tang 1996) was not needed, since errors in height adjustment are small (Bourassa et al. 2003). The Australia Antarctic Service provided three-hourly surface winds at Macquarie Island.

3. Comparison with simulated wind products

Earlier studies (Atlas et al., 1999, Ebuchi 1999) have shown that NSCAT winds are in good agreement with ECMWF and NCEP/NCAAR reanalysis winds in terms of global average. Moreover, the NSCAT provides more spatial structures than the model simulations because of its higher spatial resolution (Liu et al. 1998). Since the NSCAT era, the accuracy of QuikSCAT

winds has been improved (Liu 2002). However, a unique characteristic of the Southern Ocean is its strong and persistent wind field and rich storm activities, and scatterometer winds have not been fully validated in this area. QuikSCAT wind distributions clearly show that the winds in mid-high latitudes of the Southern Ocean (south of 30°S) significantly shifted to high wind band compared to the global wind distribution (figure 1a). Currently high wind calibration is based on the data collected during hurricanes in the low latitudes. Rain contamination imposes uncertainties on hurricane high wind observations (Stiles and Yueh 2002). The Southern Ocean makes an ideal place to evaluate scatterometer wind measurements in an environment of consistent strong winds with and without rain. Unfortunately, lack of *in situ* observations challenges scatterometer calibration. In this study, the scatterometer data are first compared with simulated surface winds. The histograms of ECMWF and QuikSCAT winds in the Southern Ocean visually indicate that satellite observations capture more high winds with speeds stronger than 15 m/s than do ECMWF simulations (figure 1b). Since these high winds only account for about 5% (4%) of total scatterometer (ECMWF) winds observed during the study period, the monthly mean wind speeds of satellite observations that are averaged over the Southern Ocean are in good agreement with model simulations, except for the period from May to October, when scatterometer winds are stronger than simulated winds (figure 2). The greatest difference between monthly mean of QSCAT-JPL and NCEP/NCAR winds reaches 0.5 m/s during austral winter. The differences between monthly QSCAT-RSS and ECMWF winds are relatively minor, representing a very small bias of 0.02 m/s for the study period. This Southern Ocean bias indicates that QuikSCAT observed stronger wind speed than do model simulations, contrasting with earlier studies showed global mean bias between NSCAT and ECMWF (-0.1~-0.2m/s) and NCEP/NCAR reanalysis (-0.1 m/s) (Atlas, et al. 1999, Ebuchi 1999). The small bias in the

Southern Ocean suggests that QuikSCAT has improved the wind speed retrieval. Among different wind products, QSCAT-JPL monthly winds are only slightly higher than QSCAT-RSS winds while ECMWF winds are slightly stronger than NCEP/NCAR winds in general.

However, the discrepancy between QuikSCAT and simulated winds becomes more pronounced when we examine high wind bands. The scatterometer observed more high wind events and its wind speeds averaging in the range of 15 m/s and higher are consistently stronger than ECMWF and NCEP/NCAR winds throughout all seasons. (figure 3a,b). The mean high wind speeds of QSCAT-RSS are about 1 m/s higher than model simulated winds, while the mean QSCAT-JPL winds are about 0.4 m/s higher than simulated winds in average. Moreover, QuikSCAT observed many more extremely strong winds (speed > 20 m/s) than do model simulations. The differences between scatterometer and simulated wind speeds reach 2 m/s for QSCAT-RSS winds and 1 m/s for QSCAT-JPL winds in this extremely high wind band (figure 3c,d).

Next, we examine the spatial distribution of the discrepancies between QSCAT-RSS and ECMWF winds. Particularly large discrepancies are found in the westerly regions of the South Indian Ocean, south of Australia and southwest of Atlantic during austral winter. Some significant differences are also found in the westerly region and near ice edge during austral autumn (figure 4). The mean RMS of wind speed differences (averaged over the Southern Ocean) varies from 1.7 m/s in summer to 2.1 m/s in winter, comparable to the global average (Atlas, et al., 1999; Ebuchi 1999). Evaluating wind direction, on the other hand, averaged over the Southern Ocean but throughout all seasons yields a mean RMS difference of 33 degrees.

Moreover, the RMS of wind direction differences is minimal in the westerly regions where large RMS wind speed differences occur, suggesting that the ambiguity of wind direction from the scatterometer winds is small in the strong wind regions. Large RMS of wind direction differences occurs in the areas where winds are weak, such as north of 40°S, particularly in austral summer and spring. Interesting enough, in these regions and seasons the wind speed differences are very small. Some extremely large RMS of wind direction differences is found near ice edge and continent coast likely due to land contamination (figure 5).

The discrepancies between QuikSCAT and simulated winds could come from two sources. First, model simulated winds may underestimate surface wind strength since the models run on much lower resolutions than the satellite footprint, and because wind observations input to the simulations are very sparse in the Southern Ocean. Second, scatterometers may overestimate the wind strength in the high wind band due to high wind saturation (Donelan and Pierson 1987). To isolate the error source, the QuikSCAT and ECMWF winds are further compared with the winds measured at the Macquarie Island Weather Station.

4. Comparison with winds in the weather station

We collocate the QSCAT-RSS winds and weather station winds by extracting the wind cells from each satellite swath pass that fell in a circular area of 18 km radius centered at the weather station. QuikSCAT usually passes this area in about 7 seconds twice daily. If multiple wind cells were extracted from one swath pass, the mean u , v , time, and distance to the station are then calculated. The number of cells extracted from a single swath pass varies from 1 to 4.

Most selected wind cells are 10 to 17 km away from the weather station, yielding a mean distance of 13km. The selected and averaged wind for each pass is then paired with the weather station wind in the nearest hour, yielding 643 (615) pairs of winds for QSCAT-RSS (QSCAT-JPL). The largest temporal difference between collocated winds reaches 90 minutes. In the meantime, ECMWF six hourly surface winds at the nearest grid point (54°, 24'S, 158°, 38'E) are also selected for comparison.

The mean difference between 643 pairs of weather station and QSCAT-RSS winds, for example, yields 0.37 m/s (suggesting stronger scatterometer winds) during the study period. This bias comes mainly from situations where paired scatterometer and weather station winds have extremely large discrepancies. Only about half of those erroneous situations fall into the high wind band. Many factors may account for these large discrepancies between collocated winds, such as high frequency wind variability (gusts), spatial variability due to inexact co-location, and other unknown reasons. To eliminate those erroneous comparisons, the data pairs with absolute differences larger than two standard deviations of the differences series (accounting for less than 5% of the samples) are deleted from the collocated dataset. The resulting dataset yields a negligible bias (-0.02 m/s). A scatter plot shows that scatterometer and weather station winds are in a good agreement after erroneous data pairs are removed (figure 6).

To further examine the wind speed bias at the high wind band, high wind (speed > 15 m/s) series are generated from collocated wind products. Table 1 lists the mean speed differences between these high wind series at Macquarie Island and the mean high wind differences between QuikSCAT and ECMWF winds over the entire Southern Ocean. All the mean high wind

differences listed in the table are significant at 99.5% confidence level except the one between QSCAT-RSS and weather station winds when erroneous points are taken out; the confidence level of the latter is reduced to 95% level. A few points stand out from this table: first, the scatterometer observes stronger high winds than that of the weather station and model simulations in most cases. Second, the weather station observes stronger wind speed than the ECMWF simulations. Third, the bias between the scatterometer and weather station high winds is much smaller relative to the bias between QuikSCAT and ECMWF high winds, and the bias between weather station and ECMWF high winds, particularly after the erroneous points are removed. Finally, the mean weather station high winds is even stronger than that of QSCAT-JPL mean high winds, and stronger than QSCAT-RSS high winds when erroneous points are removed. These results clearly indicate that ECMWF simulation underestimates the high wind strength.

In terms of the monthly mean wind speed, the QuikSCAT agrees relatively well with the ECMWF and weather station winds (figure 7a). Even the monthly high wind (speed > 15 m/s) occurrence and high wind speed are consistent between weather station and QuikSCAT winds, while ECMWF high wind speeds are somewhat lower (figure 7 b,c). Contrasted to the Southern Ocean average (figure 3), QuikSCAT winds at this location reveal no systematic monthly bias against the weather station winds, suggesting that QuikSCAT does not consistently overestimate the monthly averaged wind speed at the high wind band. The removing erroneous data pairs does not change the results from the monthly mean comparison, suggesting relatively consistent high wind speeds for weather station and QuikSCAT winds. On the other hand, monthly mean ECMWF high winds are usually lower than the other two wind products (figure 7c).

5. Impact of high winds on energy fluxes

Although high winds, particularly extremely strong winds (less than 1% of daily coverage), occur sporadically, the cumulative impact on the air-sea coupled system is significant. For example, seasonally averaged storm track intensity (approximated by $v'v'$) has shown apparent differences between ECMWF and QuikSCAT winds over most parts of the Southern Ocean. The scatterometer observes much stronger synoptic storm activities than does the model simulation. For example, the model simulation misses an important storm track in the Southern Indian Ocean near 55°S and south of Africa in the austral winter 2000 (figure 8). Consequently, scatterometer has observed much stronger surface kinetic energy fluxes approximated by the friction velocity cube (u_*^3), particularly in the South Indian Ocean and South Pacific (figure 9). In these areas, QuikSCAT observes up to 50% more energy flux than that of ECMWF. The differences between scatterometer observations and model simulations are more profound in austral fall and winter.

6. Summary

This study validates the QuikSCAT winds against ECMWF analysis and NCEP/NCAR reanalysis winds in the Southern Ocean, as well as against *in situ* wind observations from the Macquarie Island Weather Station from September 1999 to December 2000. Two QuikSCAT products from the QSCAT-1 model function and Ku-2001 model function are used. The Southern Ocean is a unique geophysical region with persistent strong winds over a huge open ocean, and rich cyclone activities. This study investigates the discrepancy between QuikSCAT and model simulations at different wind speed bands and finds that QuikSCAT observed higher

wind speed than model simulations, particular at the high wind band. The weather station data are then used to decide if QuikSCAT overestimates, or model simulations underestimate, the surface winds.

Even though the monthly mean QuikSCAT winds averaged over the Southern Ocean are in relatively good agreement with ECMWF and NCEP/NCAR winds, satellite observed wind distributions are significantly different than model simulated winds at synoptic time scales. These discrepancies are functions of space and season. There is an inverse relationship between discrepancies in wind speed and those in wind direction. For example, the largest wind speed discrepancy between scatterometer and simulated winds occurs in the westerly regions of the South Indian Ocean, the Southeast Atlantic and south of Australia; the discrepancy is most profound during austral winter and autumn. The wind direction discrepancy, however, is minimal in these regions and seasons. The largest wind direction discrepancy exists in the regions north of 40°S in austral summer and spring where and when the wind speed discrepancy is minimal.

The most significant discrepancy in wind speed comes from the high wind band (speed > 15 m/s). QuickSCAT observes more strong wind events and its mean high wind speed is greater than both ECMWF and NCEP/NCAR winds. Monthly mean high wind differences between scatterometer and reanalysis consistently reach 1-2 m/s for winds with speeds higher than 20 m/s throughout all the seasons. Although the high wind (speed > 15 m/s) and extremely high wind (speed > 20 m/s) only account for 5% and 1% of the total wind observations, respectively, during the studying period, they have a significant impact on the storm track intensity and energy flux across the air-sea interface. In particular, the scatterometer observes much stronger storm

activities and stronger energy fluxes than model simulations in austral fall and winter. In regions such as the South Indian Ocean, the strength of storm activities and kinetic energy fluxes observed by the scatterometer is up to 50% stronger than the model simulations. Therefore, accurate wind measurements are crucial in the climate studies.

In situ measurements at the weather station on Macquarie Island are used to cross validate both QuikSCAT and model simulated winds. The results reveal no systematic bias between *in situ* winds and satellite observations in both monthly mean and monthly average of high wind speeds, while weather station winds and QuikSCAT winds are consistently higher than ECMWF winds at the same location within the high wind band. This study concludes that model simulations underestimate high wind strength in the South Ocean. Low spatial model resolution and limited *in situ* observations input into the models likely cause the weaker high wind strength in the simulations. On the other hand, the modern backscatter retrieval methods provide rather good estimates at the high wind band, although there is still room for improvement. More importantly, scatterometer observations provide critical surface wind measurements with high quality and high spatial resolution for modern climate studies, particularly in this remote but climate-important region.

Acknowledgments, The author thanks Cuihua Li, programmer, who conducted most of the analyses presented in this study. Discussion with W. T. Liu has been of great benefit. Scatterometer data were provided by the Physical Oceanography Distributed Active Archive Center at Jet Propulsion Laboratory and by the Remote Sensing System. This study is supported by NASA grant JPLCIT-1216483, Lamont-Doherty Earth Observatory contribution number XXXX.

Reference:

- Atlas, R., S. C. Bloom, R. N. Hoffman, E. Brin, J. Ardizzone, J. Terry, D. Bungato and J. C. Jusem, Geophysical validation of NSCAT winds using atmospheric data and analyses. *J. Geophys. Res.*, 104, 11405-11424, 1999.
- Bourassa, M. A., D. M. Legler, J. J. O'Brien, and S. R. Smith, SeaWinds validation with research vessels. *J. Geophys. Res.*, 108 (C2), Art. No. 3019, 2003.
- Donelan, M. A. and W. J. Pierson, Radar scattering and equilibrium ranges in wind-generated waves with application to scatterometry. *J. Geophys. Res.*, 92, 4971-5029, 1987.
- Donnelly, W. J., J. R. Carswell, R. E. McIntosh, P. S. Chang, J. Wilkerson, f. Marks, and P. G. Black, Revised ocean backscatter models at C and Ku band under high-wind conditions. *J. Geophys. Res.* 104, 11,485-11,497, 1999.
- Ebuchi, N., Statistical distribution of wind speeds and directions globally observed by NSCAT. *J. Geophys. Res.*, 104, 11393-11403, 1999.
- Jones, W. L., V. Cardone, W. J. Pierson, J. Zec, L. P. Rice, A. Cox, and W. B. Sylvester, NSCAT high-resolution surface wind measurements in Typhoon Voilet, *J. Geophys. Res.*, 104, 11,247-11,259, 1999.
- Liu, W. T., Progress on Scatterometer Application, *J. of Oceanog.* Vol., 58, 121-136, 2002.
- Liu, W. T., W. Tang, and P. S. Polito, NASA scatterometer provides global ocean-surface wind fields with more structures than numerical weather prediction. *Geophys. Res. Lett.*, 25, 761-764, 1998.

- Liu, W. T. and W. Tang, Equivalent Neutral wind, JPL Pub. 96-17, Jet Propulsion Laboratory, Pasadena, 16pp, 1996.
- Kalnay, E., et al., "The NCEP/NCAR 40-year reanalysis project," *Bulletin of the American Meteorological Society*, 1996.
- Kistler, R. et al., The NCEP-NCAR 50-year reanalysis: monthly means CD-ROM and documentation. *Bull. Am. Meteor. Soc.*, 82, 247-268, 2001.
- Sharp, R. J., M. A. Bourassa, and J. O'Brien, Early detection of tropical cyclones using seawind-derived vorticity, *Bull. of Amer. Meteor. Socie.*, 83 (6), 879-889, 2002.
- Stiles, B. W. and S. H. Yueh, Impact of rain on spaceborne Ku-band wind scatterometer data, *IEEE Trans., Geosci. Remote Sens.*, 40(9), 1973-1983, 2002.
- Trenberth, K.E., *Global analyses from ECMWF and atlas of 1000 to 10 mb circulation statistics*. Tech. Rep. NCAR/TN-373+STR, National Center for Atmospheric Research, Boulder, Colorado, 1992.
- Trenberth, K. E., J. C. Berry and L. E. Buja, Vertical interpolation and truncation of model-coordinate data. NCAR/TN-396+STR, 1993.
- Wentz, F. J., D. K. Smith, C. A. Mears, and C. L. Gentemann, Advanced algorithms for QuikSCAT and SeaWinds/AMSR, *Proc. Of IGARSS 2001*, IEEE (in press).
- Yueh, S. H., R. West, F. K. Li, W. Y. Tsai and R. Lay, Dual-polarized Ku-band backscatter signatures of hurricane ocean winds. *IEEE Trans. Geosci. Remote Sens.*, 38, 73-88, 2000.
- Yueh, S. H., B. Stiles, W.-Y. Tsai, H. Hu and W. T. Liu, QuikSCAT geophysical model function for tropical cyclones and application to Hurricane Floyd. *IEEE Trans. Geosci. Remote Sens.*, 39 (12), 2601-2612, 2001.

Zeng, L. and G. Levy, 1995, Space and time aliasing structure to monthly mean polar-orbiting satellite data. *J. Geophys. Res.*, 100, 5133-5142, 1995.

Figure Captions

Figure 1 Wind speed histogram for the global and Southern Ocean (30°S to ice edge) ECMWF surface winds (a) and wind speed histogram for the Southern Ocean observed by QuikSCAT and simulated by ECMWF (b).

Figure 2 Monthly wind speeds (m/s) averaged over the Southern Ocean from September 1999 to December 2002 from QSCAT-RSS (dotted line) and QSCAT-JPL (dot-dashed line) as well as from NCEP/NCAR reanalysis (dashed line) and ECMWF operational analysis (solid line).

Figure 3 Monthly high wind (speed > 15 m/s) occurrence (a) and mean high wind speed (b) together with extremely strong wind (speed > 20 m/s) occurrence (c) and their mean speed (d) in the Southern Ocean from September 1999 to December 2000 observed by the satellite and simulated by models.

Figure 4 Seasonal RMS daily wind speed differences between QSCAT-RSS and ECMWF winds (m/s).

Figure 5 Seasonal RMS daily wind direction differences between QSCAT-RSS and ECMWF winds (degree).

Figure 6 Scatter plot of QSCAT-RSS and weather station observed wind speeds after erroneous data pairs were removed. Black line is the linear regression. The blue and red lines are the 95% confidence level for the regression line and regression points, respectively.

Figure 7 Monthly mean surface wind speeds (m/s) at Macquarie Island observed by the weather station (dashed lines), QSCAT-RSS (dotted lines) and simulated by ECMWF (solid lines) from September 1999 to December 2000 (a). High wind (speed > 15 m/s) occurrence and mean high wind speeds are also plotted (b & c).

Figure 8 Seasonal storm track intensity approximated by averaging daily $v'v'$ (m^2/s^2) from ECMWF (left column) and QSCAT-RSS (right column) winds in austral fall and winter 2000.

Figure 9 Seasonal u_*^3 calculated from daily ECMWF (left column) and QSCAT-RSS (right column) winds in austral fall and winter, 2000.

Table 1. Mean High Wind Differences between Different wind Products

	Bias		Bias without erroneous points	
	QSCAT-RSS	QSCAT-JPL	QSCAT-RSS	QDCAT-JPL
QuikSCAT – Weather Station	0.62	-0.11	-0.03	0.20
Weather Station – ECMWF	0.86		0.77	
QuikSCAT – ECMWF (at Macquarie Island)	1.11	0.65	0.44	0.46
QuikSCAT – ECMWF Over Southern Ocean	1.11	0.39	0.49	0.29

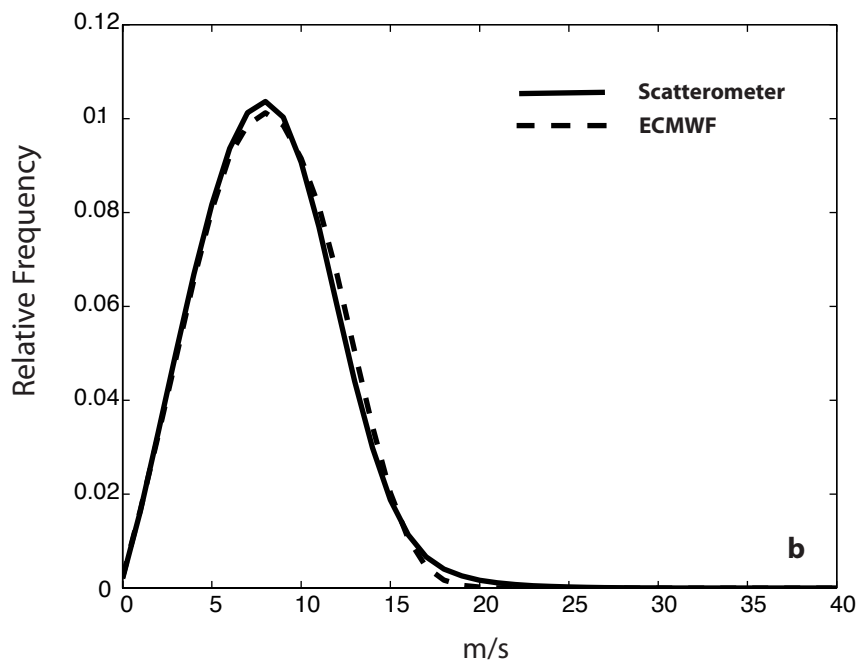
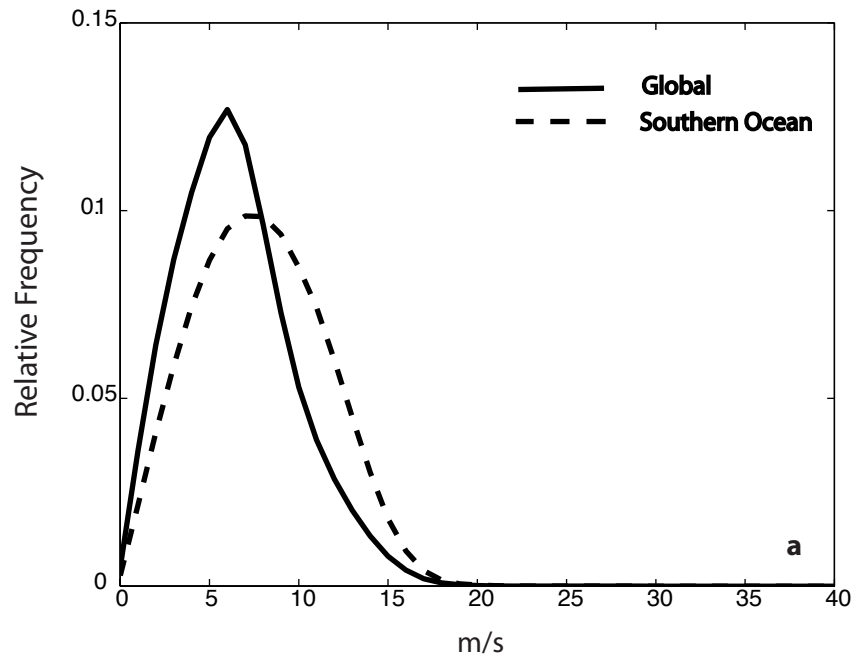


Figure 1 Wind speed histogram for the global and Southern Ocean (30°S to ice edge) ECMWF surface winds (a) and wind speed histogram for the Southern Ocean observed by QSCAT-RSS and simulated by ECMWF (b).

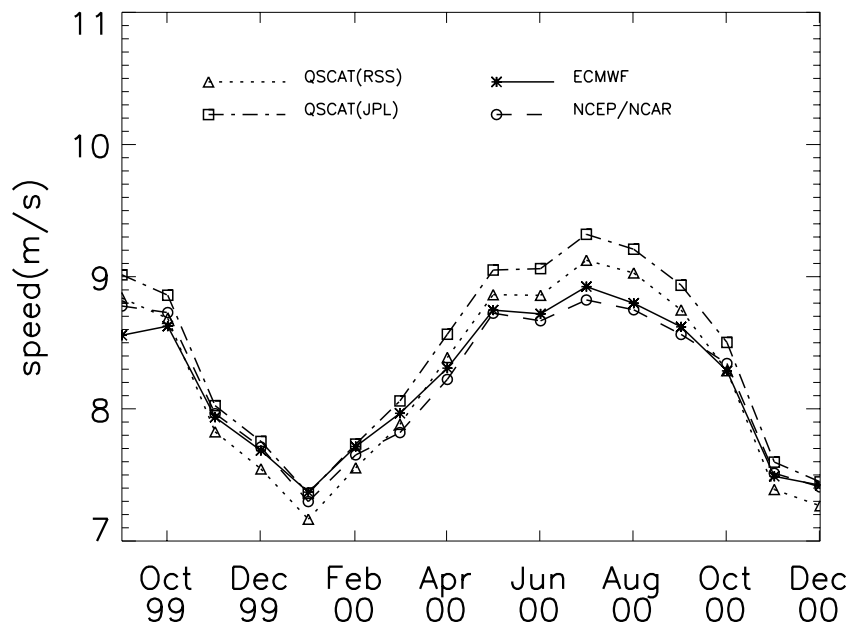


Figure 2 Monthly wind speeds (m/s) averaged over the Southern Ocean from September 1 999 to December 2002 from QSCAT-RSS (dotted line) and QSCAT-JPL (dot-dashed line) as well as from NCEP/NCAR reanalysis (dashed line) and ECMWF operational analysis (solid line).

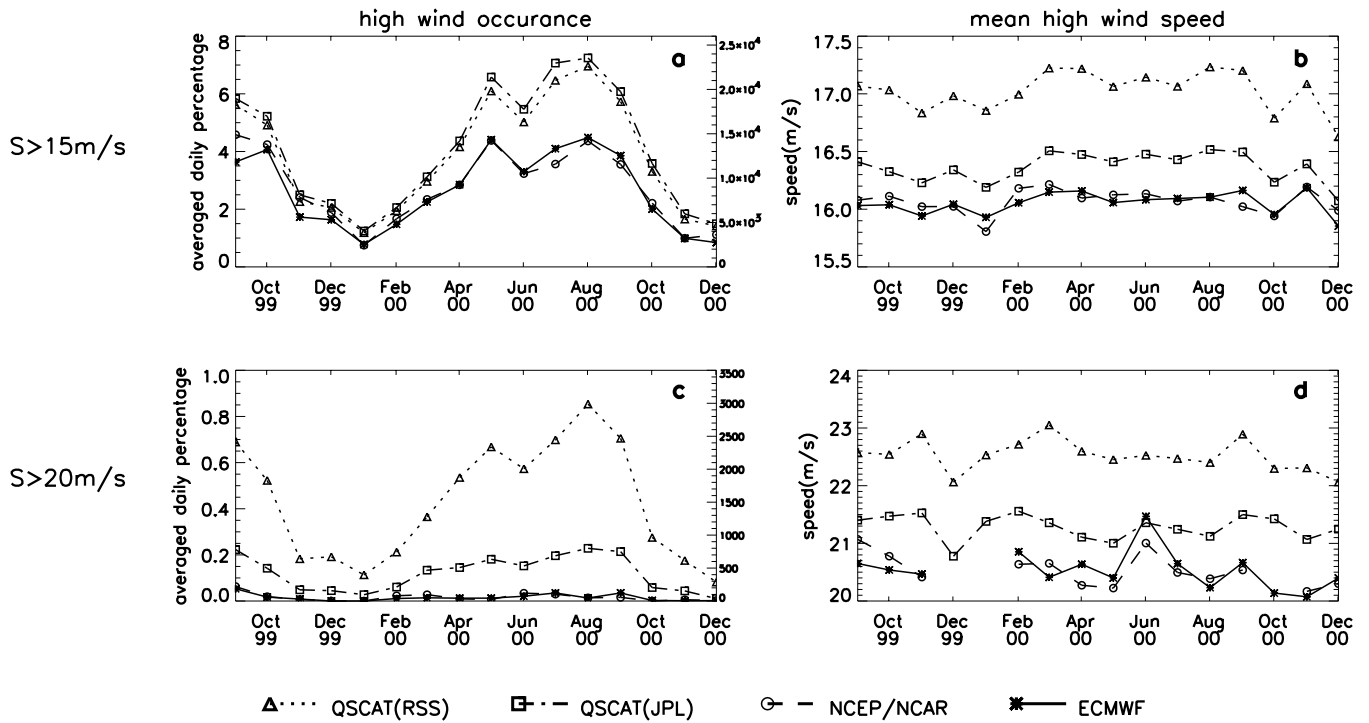


Figure 3 Monthly high wind (speed $> 15 \text{ m/s}$) occurrence (a) and mean high wind speed (b) together with extremely strong wind (speed $> 20 \text{ m/s}$) occurrence (c) and their mean speed (d) in the Southern Ocean from September 1999 to December 2000 observed by the satellite and simulated by models.

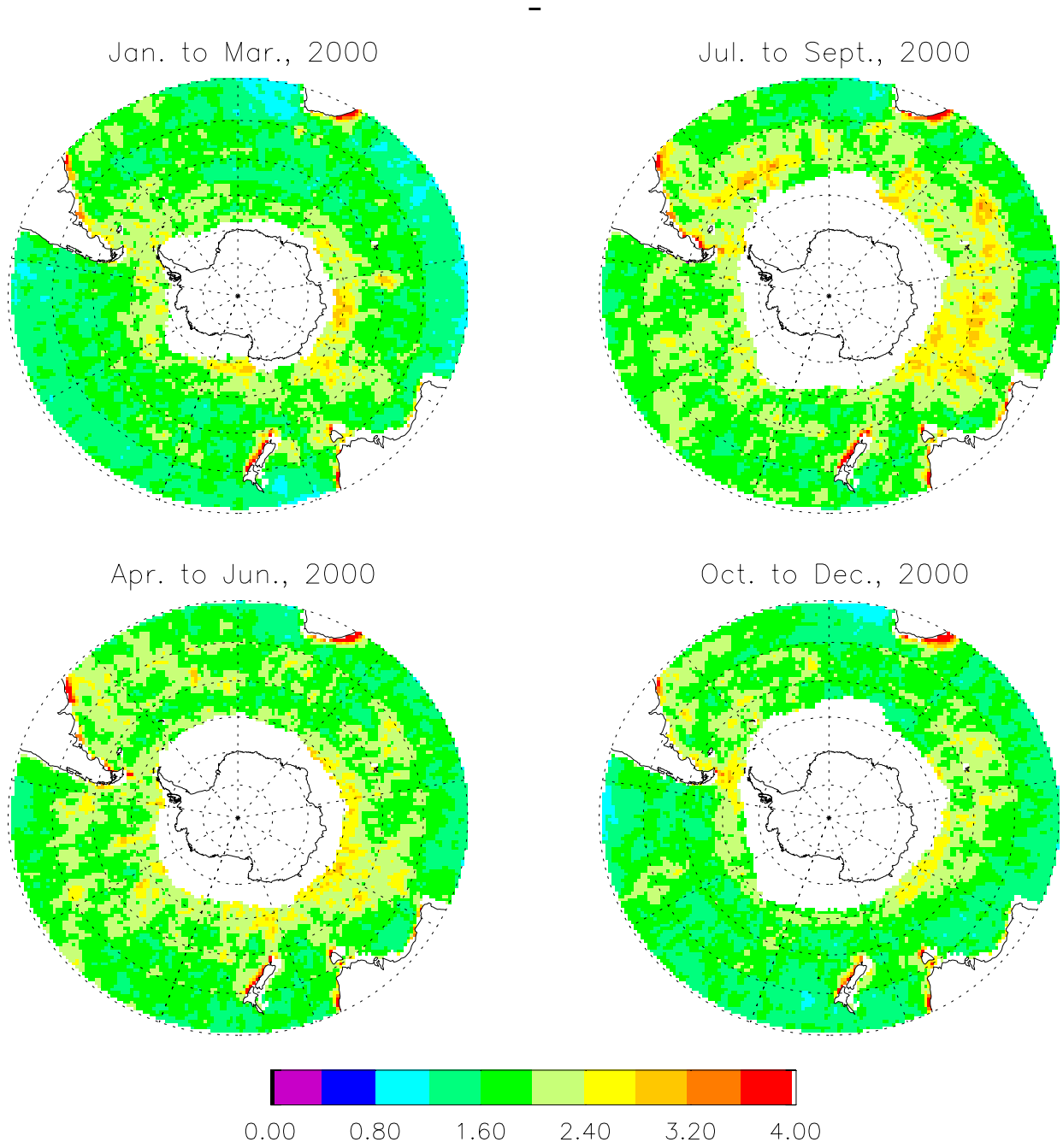


Figure 4 Seasonal RMS daily wind speed differences between QSCAT-RSS and ECMWF winds (m/s).

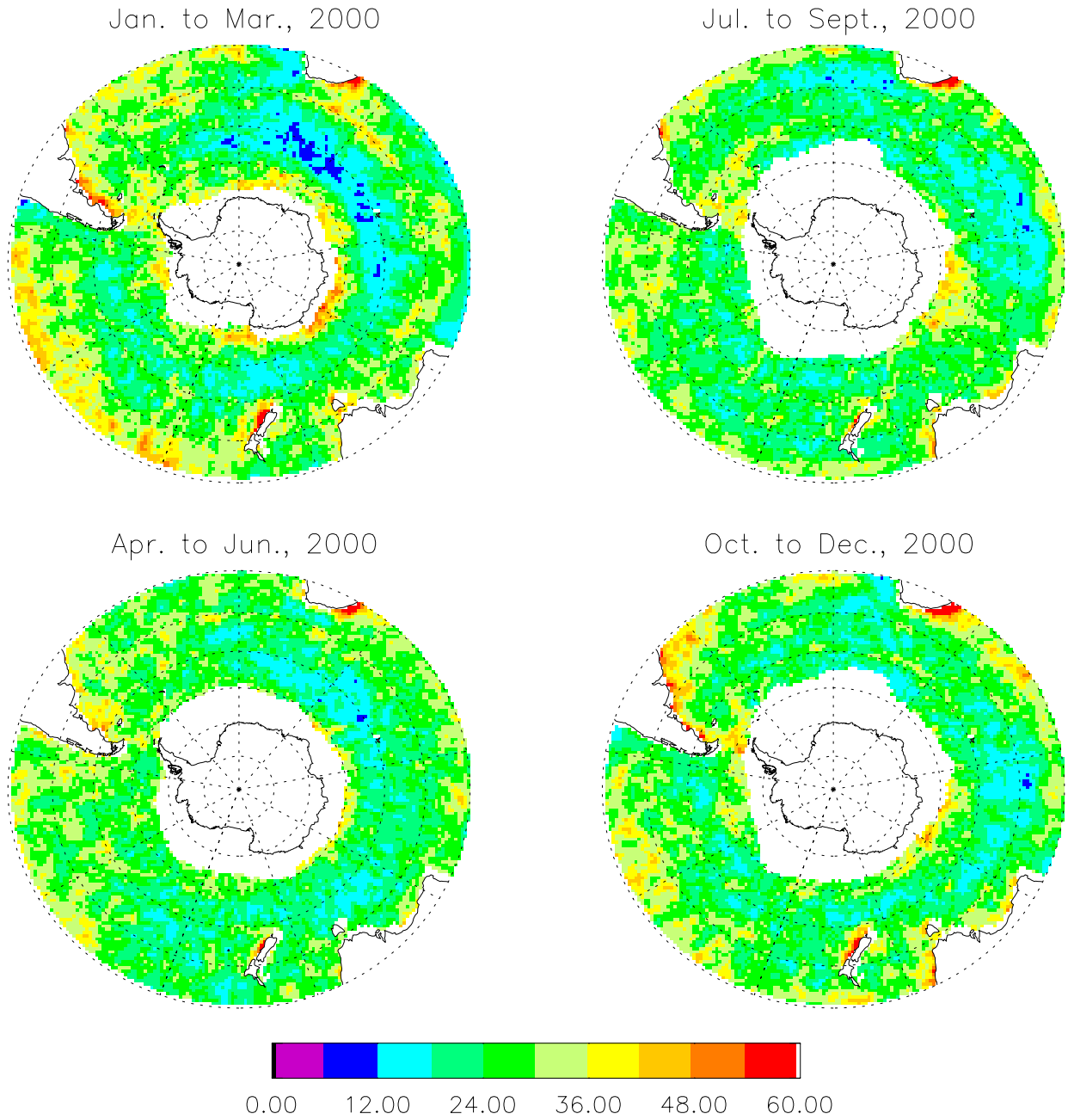


Figure 5 Seasonal RMS daily wind direction differences between QSCAT-RSS and ECMWF winds (degree).

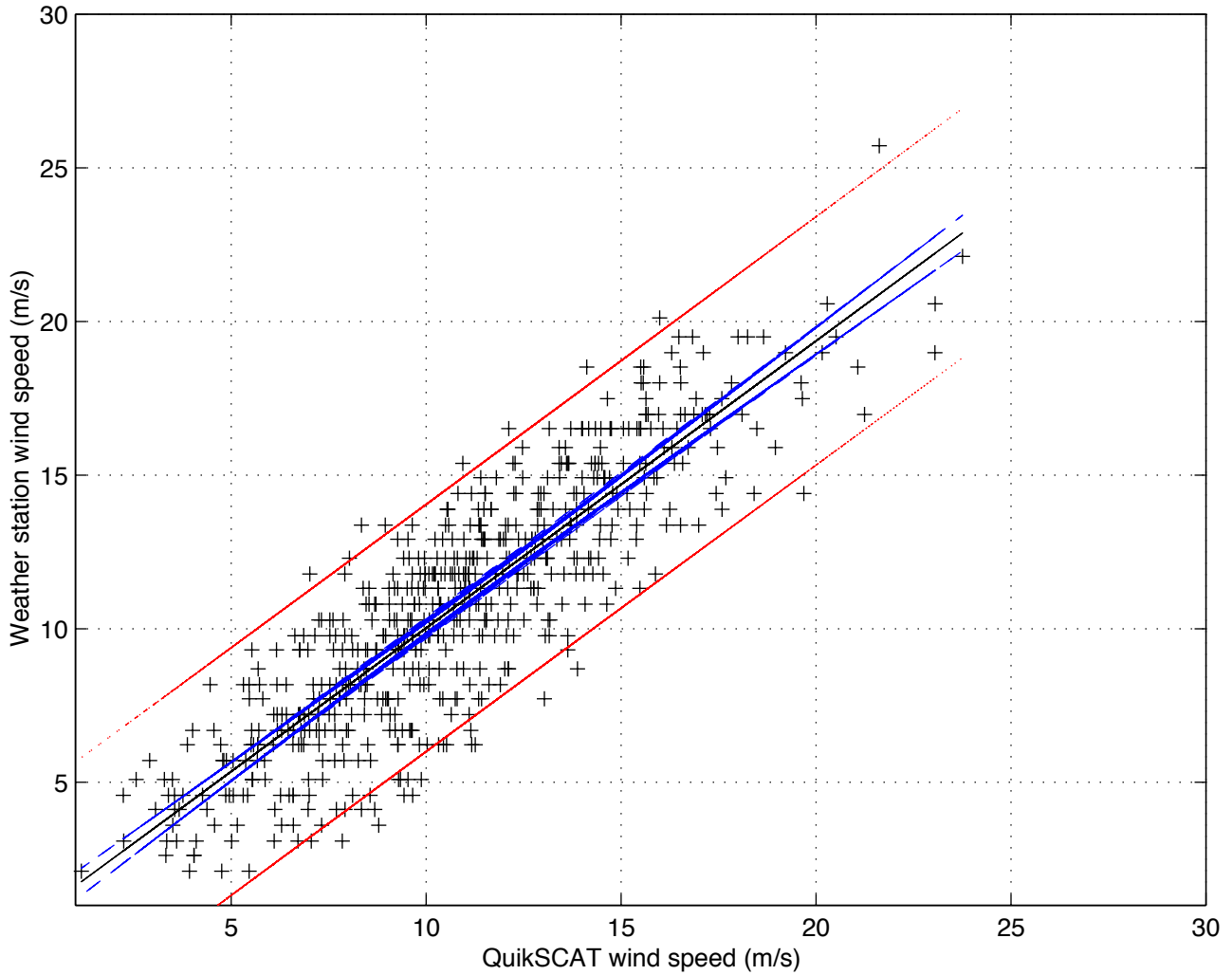


Figure 6 Scatter plot of QSCAT-RSS and weather station observed wind speeds after erroneous data pairs were removed. Black line is the linear regression. The blue and red lines are the 95% confidence level for the regression line and regression points, respectively

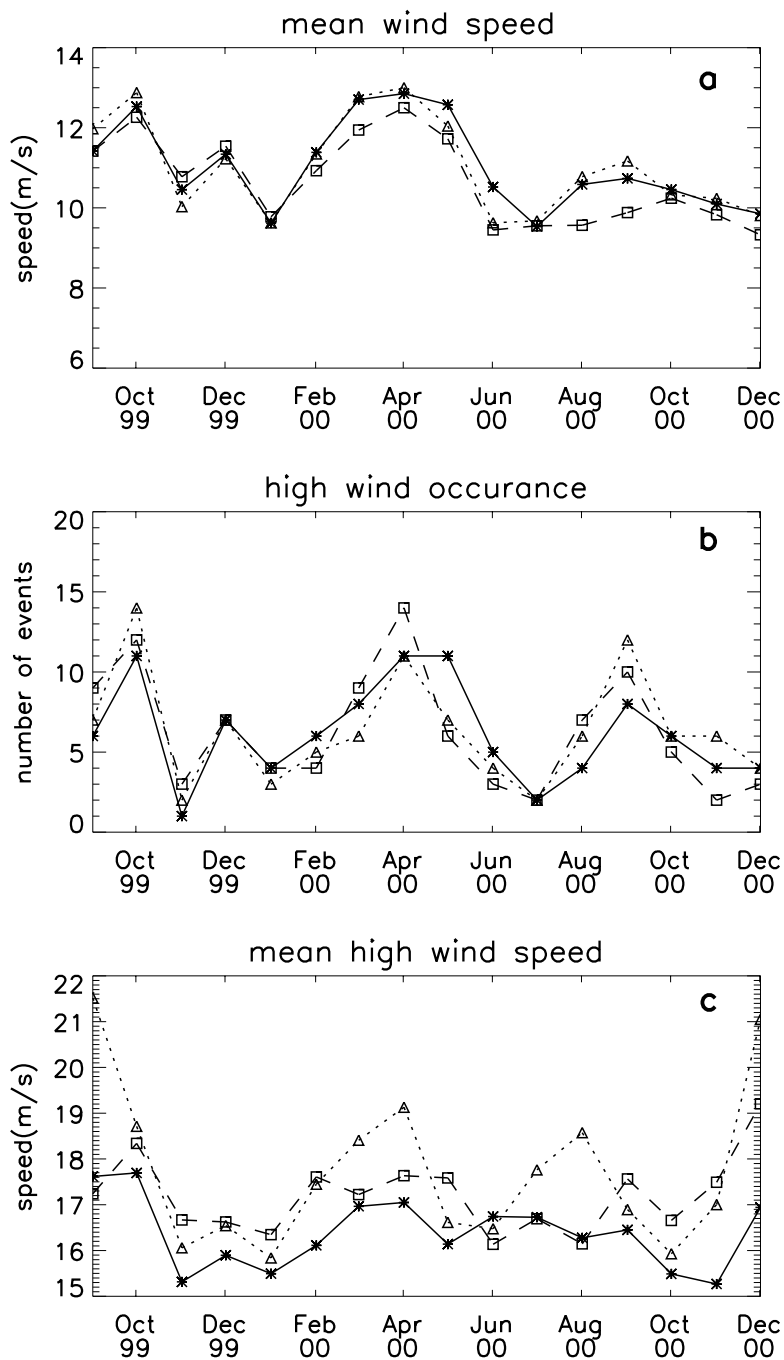
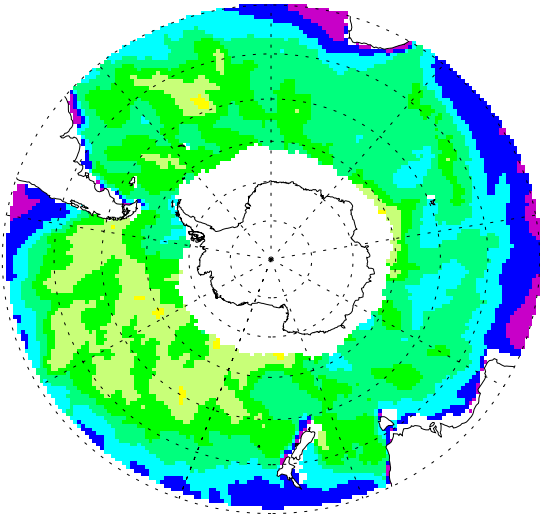


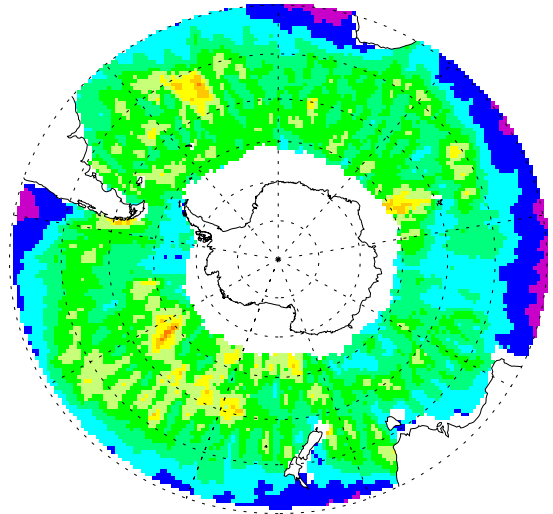
Figure 7 Monthly mean surface wind speeds (m/s) at Macquarie Island observed by the weather station (dashed lines), QSCAT-RSS (dotted lines) and simulated by ECMWF (solid lines) from September 1999 to December 2000 (a). High wind (speed > 15 m/s) occurrence and mean high wind speeds are also plotted (b & c).

Seasonal Mean of $v'v'$

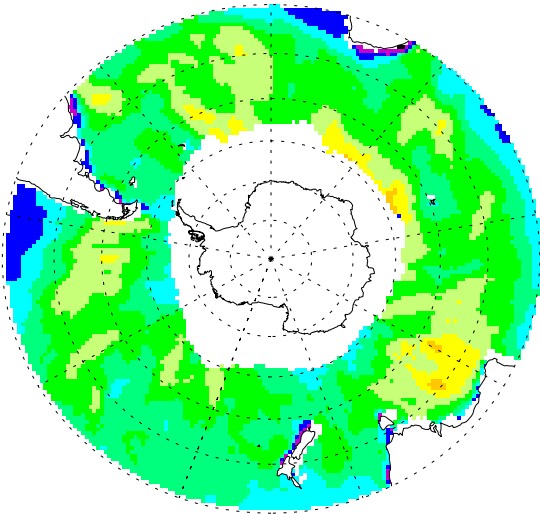
Mar. to May, 2000(ECMWF)



Mar. to May, 2000(QSCAT,RSS)



Jun. to Aug., 2000(ECMWF)



Jun. to Aug., 2000(QSCAT,RSS)

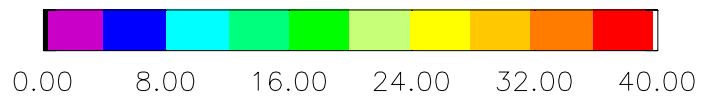
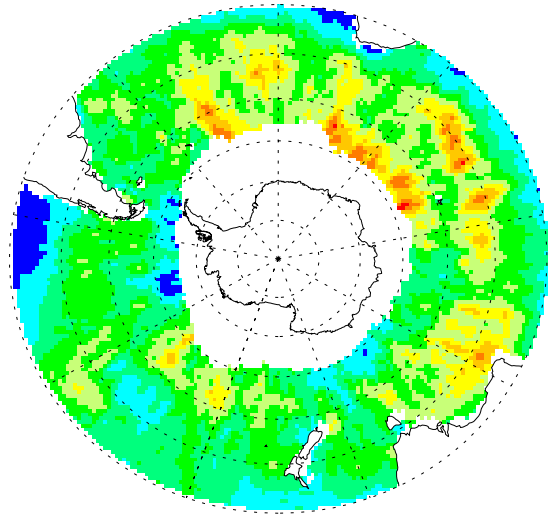
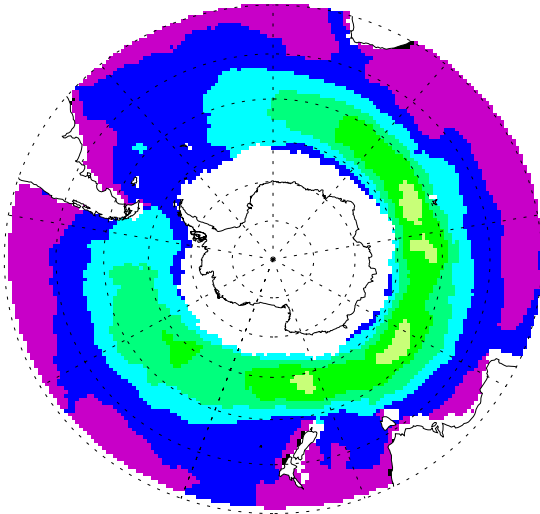
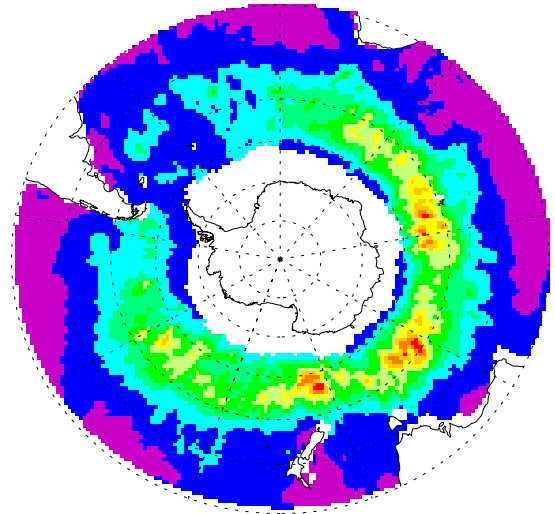


Figure 8 Seasonal storm track intensity approximated by averaging daily $v'v'$ (m^2/s^2) from ECMWF (left column) and QSCAT-RSS (right column) winds in austral fall and winter 2000.

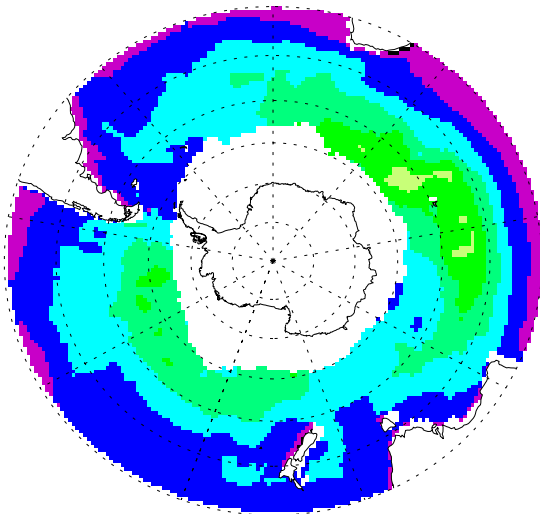
Mar. to May, 2000(ECMWF)



Mar. to May, 2000(QSCAT,RSS)



Jun. to Aug., 2000(ECMWF)



Jun. to Aug., 2000(QSCAT,RSS)

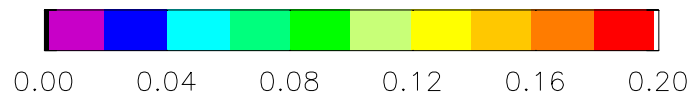
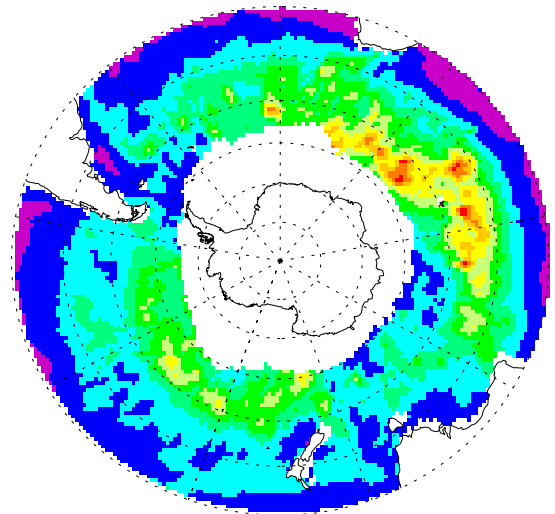


Figure 9 Seasonal u^*3 calculated from daily ECMWF (left column) and QSCAT-RSS (right column) winds in austral fall and winter, 2000.